Cancer Nanotechnology

RESEARCH Open Access

Biological modeling of gadolinium-based nanoparticles radio-enhancement for kilovoltage photons: a Monte Carlo study

Jianan Wu[1*], Xiaohan Xu[1], Ying Liang[1], Tujia Chen[2], Enzhuo Quan[1] and Luhua Wang[1,3]

*Correspondence: wujianande@gmail.com

[1] Department of Radiation Oncology, National Cancer Center/National Clinical Research Center for Cancer/Cancer Hospital & Shenzhen Hospital, Chinese Academy of Medical Sciences and Peking Union Medical College, Shenzhen 518116, People's Republic of China
[2] School of Pharmaceutical Sciences, Health Science Center, Shenzhen University, Shenzhen 518060, People's Republic of China
[3] Department of Radiation Oncology, National Cancer Center/National Clinical Research Center for Cancer/Cancer Hospital, Chinese Academy of Medical Sciences and Peking Union Medical College, Beijing 100021, People's Republic of China

Abstract

Background: Gadolinium-based nanoparticles (GdNPs) are clinically used agents to increase the radiosensitivity of tumor cells. However, studies on the mechanisms and biological modeling of GdNP radio-enhancement are still preliminary. This study aims to investigate the mechanism of radio-enhancement of GdNPs for kilovoltage photons using Monte Carlo (MC) simulations, and to establish local effect model (LEM)-based biological model of GdNP radiosensitization.

Methods: The spectrum and yield of secondary electrons and dose enhancement around a single GdNP and clustered GdNPs were calculated in a water cube phantom by MC track-structure simulations using TOPAS code. We constructed a partial shell-like cell geometry model of pancreatic cancer cell based on transmission electron microscope (TEM) observations. LEM-based biological modeling of GdNP radiosensitization was established based on the MC-calculated nano-scale dose distributions in the cell model to predict the cell surviving fractions after irradiation.

Results: The yield of secondary electrons for GdNP was 0.16% of the yield for gold nanoparticle (GNP), whereas the average electron energy was 12% higher. The majority of the dose enhancement came from the contribution of Auger electrons. GdNP clusters had a larger range and extent of dose enhancement than single GdNPs, although GdNP clustering reduced radial dose per interacting photon significantly. For the dose range between 0 and 8 Gy, the surviving fraction predicted using LEM-based biological model laid within one standard deviation of the published experimental results, and the deviations between them were all within 25%.

Conclusions: The mechanism of radio-enhancement of GdNPs for kilovoltage photons was investigated using MC simulations. The prediction results of the established LEM-based biological model for GdNP radiosensitization showed good agreement with published experimental results, although the deviation of simulation parameters can lead to large disparity in the results. To our knowledge, this was the first LEM-based biological model for GdNP radiosensitization.

Keywords: Monte Carlo simulation, Local effect model, Gadolinium-based nanoparticle, Radiosensitization

Background

Cancer has been an increasingly serious threat to human health worldwide (Sung et al. 2021). About half of patients are estimated to receive radiotherapy at some point after a diagnosis of cancer (Chandra et al. 2021). Metallic nanoparticle radiosensitization (MNPR) is a potential clinical approach to potentiate the effects of radiotherapy, where metallic nanoparticles introduced into the tumor site serve as radiosensitizers. It has drawn significant attention from the research community and now several products are under clinical trials (Kempson 2021; Lux et al. 2019; Verry et al. 2019). In addition to physical mechanisms by dose enhancement, physico-chemical, chemical and biological mechanisms of radiosensitizations have been revealed by many recent studies (Chatzipapas et al. 2020; Kempson 2021; Rudek et al. 2019).

The Monte Carlo (MC) method has been widely used in radiotherapy and is considered the "gold standard" for dose calculation. Unlike the generally used MC condensed history codes in radiotherapy dosimetry at the macro scale, MC track structure codes simulate all elastic and inelastic collisions one by one at the nanometer level down to very low energies, thus offering a theoretical tool for investigating the mechanism of radiation-induced damage, calculating energy deposition at nano-scale and biological modeling (Chatzipapas et al. 2020; Wu et al. 2020).

Gold, being biocompatible and one of the heaviest stable elements, was a natural candidate for radiosensitizer; thus, most MC studies on the mechanism and biological modeling of radiosensitization used gold nanoparticles (GNPs) (Xu et al. 2022). Rudek et al. discovered that the dose enhancement was highest for GNP irradiated with keV X-rays, and much lower with MV X-rays, protons or carbon-ions; thus, for keV X-rays, the dose enhancement at the physical stage is the dominant mechanism of GNP radiosensitization (Rudek et al. 2019). Engels et al. established a radiobiological model for GNP radiosensitization under keV X-rays using MC dose calculations at nano-scale in a subcellular model based on the local effect model (LEM), and the prediction fitted well with cell experiments (Engels et al. 2020). However, the clinical translation of GNPs was stagnant.

Unlike GNPs, gadolinium-based nanoparticles (GdNPs) have been evaluated by completed phase I and II trials, thus more promising for clinical use. AGuIX, sub-5 nm GdNPs made of a polysiloxane matrix and gadolinium chelates, have been developed as an intravenously administered radiosensitizer. The radiosensitization effect of AGuIX in cancer has been evaluated in multiple cell models and mouse xenograft models (Lux et al. 2019; Du et al. 2020). Recently, AGuIX nanoparticles have been used along with radiotherapy in a phase III clinical trial for the treatment of brain metastasis (Verry et al. 2019) (Phase Ib NANO-RAD: NCT02820454 and Phase 2 NANO-RAD2: NCT03818386) and cervical cancer (Lux et al. 2019) (Phase Ib NANO-COL: NCT03308604).

While the clinical translation of GdNPs has been going well, research on the biological modeling of GdNPs was not as sufficient as that of GNPs. McMahon et al. have discovered upon MC simulations that the nano-scale dose enhancement following X-ray irradiation was not exactly positively correlated to the atomic number (with the photoelectric effect scaling as Z^3) of the radiosensitizer and that gadolinium might be a better choice of radiosensitizer than gold due to the dose contribution by secondary Auger electrons (McMahon et al. 2016). Taupin et al. established the prediction model of the

cell surviving fractions for cells incubated with GdNPs following irradiation with monochromatic keV and MV X-rays and the prediction fitted well with the experiment results using glioma cells (Taupin et al. 2015). However, this model only considered the dose enhancement at the centimeter scale. The impact of nano-scale dose enhancement with a high gradient in the sensitive volume was ignored, which could be well dealt with using LEM.

In this work, we investigated the mechanism of radio-enhancement of GdNPs for kilovoltage photons. The secondary electron spectrum, dose distributions and dose enhancement ratio (DER, i.e., the ratio of the absorbed dose with and without the GdNP) distributions at nano-scale were calculated by MC simulations for various irradiation configurations, including single GdNP, clustered GdNPs and a sub-cellular model containing GdNPs established according to cell irradiation experiment. Based on the MC calculations in the sub-cellular model, LEM-based biological modeling of GdNP radio-enhancement was established, and the prediction of cell surviving fractions was compared with experimental results.

Materials and methods

Monte Carlo code and simulation configuration

The TOPAS MC code (Perl et al. 2012) is an advanced and user-friendly extension to Geant4 (Agostinelli et al. 2003; Allison et al. 2006, 2016). TOPAS version 3.7 with Geant4 version 10.06.p03 was used in this work, as well as TOPAS-nBio (Schuemann et al. 2019) version 1.0, an extension layered on Geant4-DNA (Incerti et al. 2018) that focused on radiation biology at sub-cellular scales. For simulations containing mixed materials, TOPAS-nBio is capable of defining regions of interest, where MC track-structure simulations are activated while using the standard condensed-history MC physics modules in other regions. In this work, the MC track-structure physics module "g4em-dna_opt4" was used in water (G4_WATER) unless otherwise specified, and "g4em-penelope" was used in all the other regions. Auger effect and particle induced X-ray emission were activated in all processes of the simulations unless otherwise specified.

Modeling single gadolinium-based nanoparticle irradiation

AGuIX nanoparticles appear as single particles or clusters in tumor cells (Detappe et al. 2015). The geometry described in Fig. 1 was utilized to study the radial dose distribution for AGuIX cluster or single particle irradiation. GdNPs with diameters of 50 nm and 5 nm represented a AGuIX cluster and a single AGuIX particle, respectively (Detappe et al. 2015). The elemental fractions of the GdNPs were set according to the average chemical formula of AGuIX (Verry et al. 2020), and the density was set to 0.254 g/cm^3 derived from the diameter and mass of AGuIX (Detappe et al. 2015). The GdNP (diameter 50 nm or 5 nm) was placed at the center of a water cube with a side length of 1 μm. A 220 kVp X-ray beam perpendicular to the cube surface was employed to irradiate the cube. The X-ray spectra were generated using SpekPy (Poludniowski et al. 2021), which is shown in Fig. 2. The 1 μm cube was place at the center of a water cube with a side length of 300 μm to provide electron equilibrium. The 1 μm cube used "g4em-dna_opt4", while the 300 μm cube used "g4em-penelope". The size of the beam was large enough to reach electron equilibrium with respect to the Auger electrons released by the

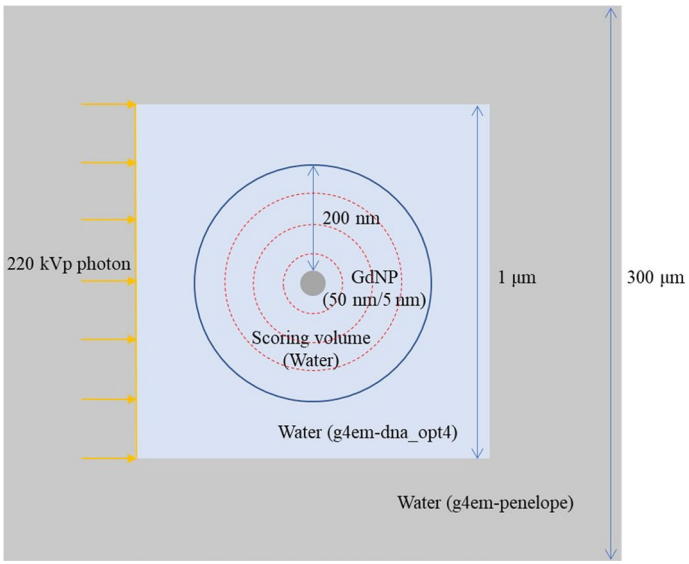

Fig. 1 Schematic view of the simulation setup for single AGuIX nanoparticle irradiation (sizes not to scale)

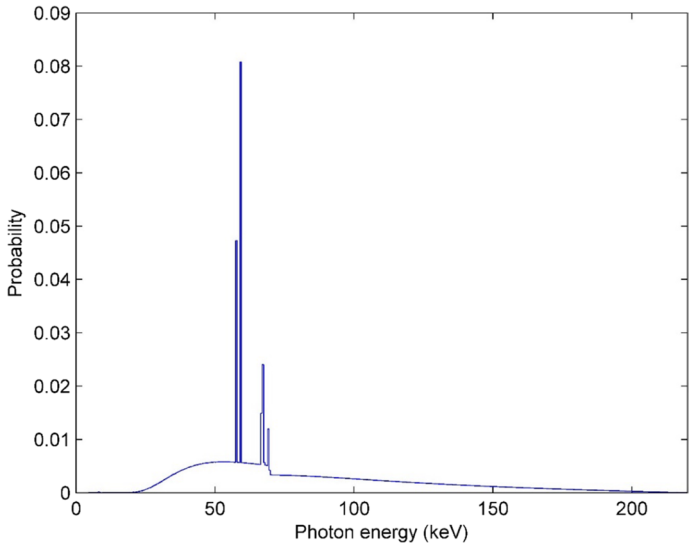

Fig. 2 220 kVp X-ray spectra (generated using SpekPy, Poludniowski et al. 2021)

nanoparticles, but not for the Compton interactions by the X-ray photons with the water medium. The radial dose distribution was scored for a distance ranging from the surface of the GdNP to 200 nm away. The scoring bin size was 1 nm for the distance from the surface to 10 nm, 5 nm for the distance from 10 to 50 nm, and 10 nm for the distance from 50 to 200 nm. The radial DER was also calculated.

Cell geometric model containing gadolinium-based nanoparticles

The cell geometric model and irradiation setup established in this research were based on a published paper (Detappe et al. 2015), as shown in Fig. 3; thus, the simulation results would be comparable to their experimental results. A partial shell-like geometric

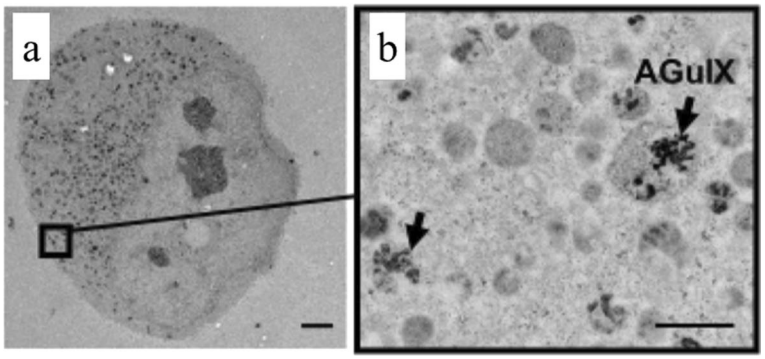

Fig. 3 Tumor cell uptake for AGuIX. Cited from a previous study (Detappe et al. 2015). **a** TEM image (3000×) depict the active endocytosis uptake of AGuIX into the Panc1 tumor cells. Bar 5 µm. **b** Magnified TEM image (25,000×) shows AGuIX nanoparticles captured by endosomal vesicles (black arrow) and carried into the cytoplasm. Bar 1 µm

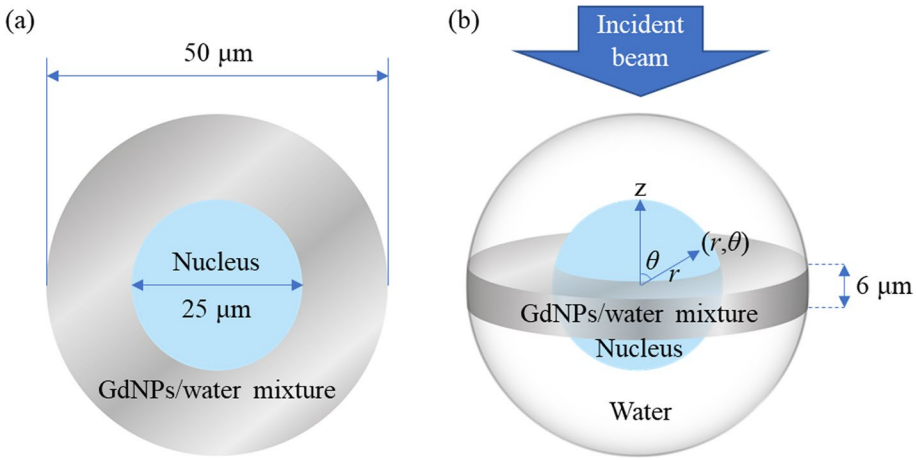

Fig. 4 Partial GdNP shell configuration used in the simulation. **a** Beam view, **b** Perspective view

cell configuration was adopted in this study (Fig. 4), which was inspired by previously published works (Engels et al. 2020; Liu et al. 2019). In this configuration, the gadolinium and water mixture are distributed evenly in the cytoplasm with the top and bottom of the nucleus uncovered, forming a partial shell. The gadolinium content in the cytoplasm was set according to the experimental measurement (1.25 pg of AGuIX per cell). Transmission electron microscope (TEM) imaging reveals that after 1 h of incubation, the nanoparticles are predominantly localized in vacuoles in the cytoplasm, with the top and bottom of the nucleus uncovered, as shown in Fig. 3a, b. Therefore, our geometry mimics the average GdNP distribution surrounding the nucleus in TEM images in a simplistic way. According to TEM images, the diameters of the cell and the nucleus were set to 50 µm and 25 µm, respectively. The height of the partial shell was set to 6 µm following Engels et al. (Engels et al. 2020). A 220 kVp X-ray beam perpendicular to the partial–shell was employed to irradiate the cell model for a dose range of 2–10 Gy to mimic Detappe's experiment. Using the simulation configuration illustrated in Fig. 4, the dose distribution in the nucleus for the irradiated cellular model was obtained by MC calculation and expressed as $D(r,\theta)$ in the spherical coordinate system shown in Fig. 4.

LEM-based biological modeling of GdNP radio-enhancement

LQM (McMahon 2018) relates the average dose delivered to the cell (D) to the cell surviving fraction (S), as shown in Eq. (1)

$$S = \exp\left[-\left(\alpha D + \beta D^2\right)\right], \tag{1}$$

where α and β can be determined by cell irradiation experiments. The LQM is well-suited to describe the effect of uniform irradiation on cell survival, whereas the impact of non-uniform irradiation was not well-described by LQM. To address this issue, several radiobiological models have been developed, including LEM, microdosimetric kinetic model (MKM), etc.

LEM was originally developed to determine the radiobiological effectiveness of heavy ion irradiation (Scholz and Kraft 1993). It was later used in the prediction of cell surviving fractions from MC simulations concerning the nanoscale dose inhomogeneity produced by GNPs (Lechtman et al. 2013; Ferrero et al. 2017; Engels et al. 2020). LEM relates the energy depositions on the nanoscale to the cell survival (S). S can be expressed as a function of the number of lethal events (N) following Poisson statistics, as shown in Eq. (2)

$$S = \exp(-N), \tag{2}$$

where N is calculated using Eq. (3)

$$N = -\int_{V_s} \frac{\ln(S(D(x,y,z)))}{V_s} \mathrm{d}V \tag{3}$$

The local dose ($D(x,y,z)$) in a sensitive volume (V_s) due to the incident irradiation field was utilized to compute a spatially dependent $S(D(x,y,z))$. The $S(D(x,y,z))$ was obtained using Eq. (1), which is evaluated at nanoscale volumes ($\mathrm{d}V$) within V_s.

To relate the energy deposition distributions ($D(r,\theta)$) on the nanoscale obtained by MC simulations using the cell model shown in Fig. 4 to the cell surviving fraction, we transformed Eq. (3) into spherical coordinate system and combined it with Eq. (1), as shown in Eq. (4)

$$N_{\mathrm{GdNP}} = \frac{1}{V_c} \int_{r=0}^{R_C} \int_{\theta=0}^{180} \left[\alpha D(r,\theta) + \beta D(r,\theta)^2\right] \mathrm{d}V \tag{4}$$

where V_C and R_C represent the volume and radius of the cellular nucleus, respectively. The cell surviving fraction of the cell model containing GdNPs (S_{GdNP}) can then be calculated using Eq. (5)

$$S_{\mathrm{GdNP}} = \exp(-N_{\mathrm{GdNP}}). \tag{5}$$

.

The DER distribution in the nucleus was defined as the ratio between the two energy deposition distributions simulated using the cell model with and without

Table 1 Properties of the secondary electrons emitted by 50 nm GdNP and GNP when irradiated by 220 kVp X-ray in vacuum

	GdNP	GNP
Number of secondary electrons per incident photon	0.000011	0.0067
Average energy of secondary electrons (keV)	3.69	3.29
Average range of secondary electrons in water (μm)	0.45	0.37

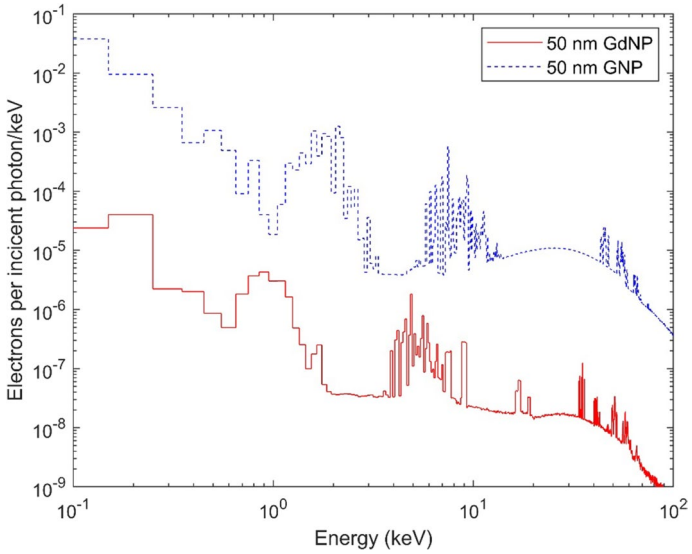

Fig. 5 Spectra of the secondary electrons emitted by 50 nm GdNP and GNP when irradiated by 220 kVp X-ray in vacuum

GdNPs. The delivered dose in the experiment (0–10 Gy) times the DER distribution to get the dose distribution in the radio-sensitized nucleus.

The LQM fitting of S_{GdNP} gets the effective dose (D_{eff}), as shown in Eq. (6)

$$S_{\mathrm{GdNP}} = \exp\left[-\left(\alpha D_{\mathrm{eff}} + \beta {D_{\mathrm{eff}}}^2\right)\right] \tag{6}$$

.

The effective DER ($\mathrm{DER}_{\mathrm{eff}}$) is defined as D_{eff}/D_0, where D_0 is the experimental delivered dose. The average DER ($\mathrm{DER}_{\mathrm{av}}$), on the other hand, is defined as D_{av}/D_0, where D_{av} is the average dose in the nucleus.

Results

Single GdNP irradiation

Irradiated with a circular planar 220 kVp X-ray source with a diameter of 50 nm in vacuum, the secondary electron spectra emitted by 50 nm GdNP in comparison with the spectra of 50 nm GNP are shown in Fig. 5. The properties of the secondary electrons emitted by GdNP and GNP in vacuum are shown in Table 1. Using the simulation setup illustrated in Fig. 2, we obtained the radial dose distributions of 50 nm and 5 nm GdNP under irradiation of the simulated spectrum, which were normalized to dose per

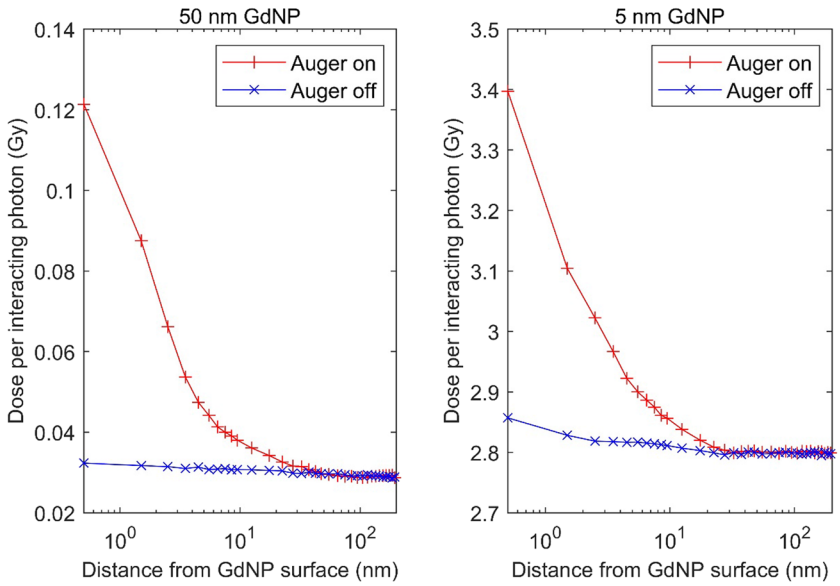

Fig. 6 Radial dose distribution around the irradiated GdNP with a diameter of 50 nm and 5 nm, respectively

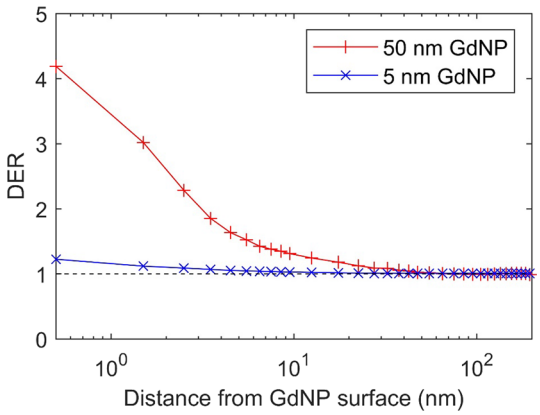

Fig. 7 Radial DER around the irradiated GdNP with a diameter of 50 nm and 5 nm, respectively

interacting photon with the GdNP (Fig. 6). The radial DER of 50 nm and 5 nm irradiated GdNPs is shown in Fig. 7.

Dose deposition and DER in cellular model

The dose and DER distributions on half of the cross section of the nucleus are shown in Fig. 8a, b, respectively. The dose distribution was also plotted as a function of the radial distance from the center of the nucleus as well as the polar angle θ, as shown in Fig. 8c. Note that all plots in Fig. 8 were in logarithmic color scale. The dose profile along the 90-degree radial axis of the cross section of the nucleus [dashed line in Fig. 8a] is illustrated in Fig. 9. On average, the dose deposition per incident photon for the cellular model containing gadolinium was 4.4722×10^{-9} Gy, while for the cellular model without gadolinium it was 4.2088×10^{-9} Gy, resulting in a DER_{av} in the nucleus of 1.063.

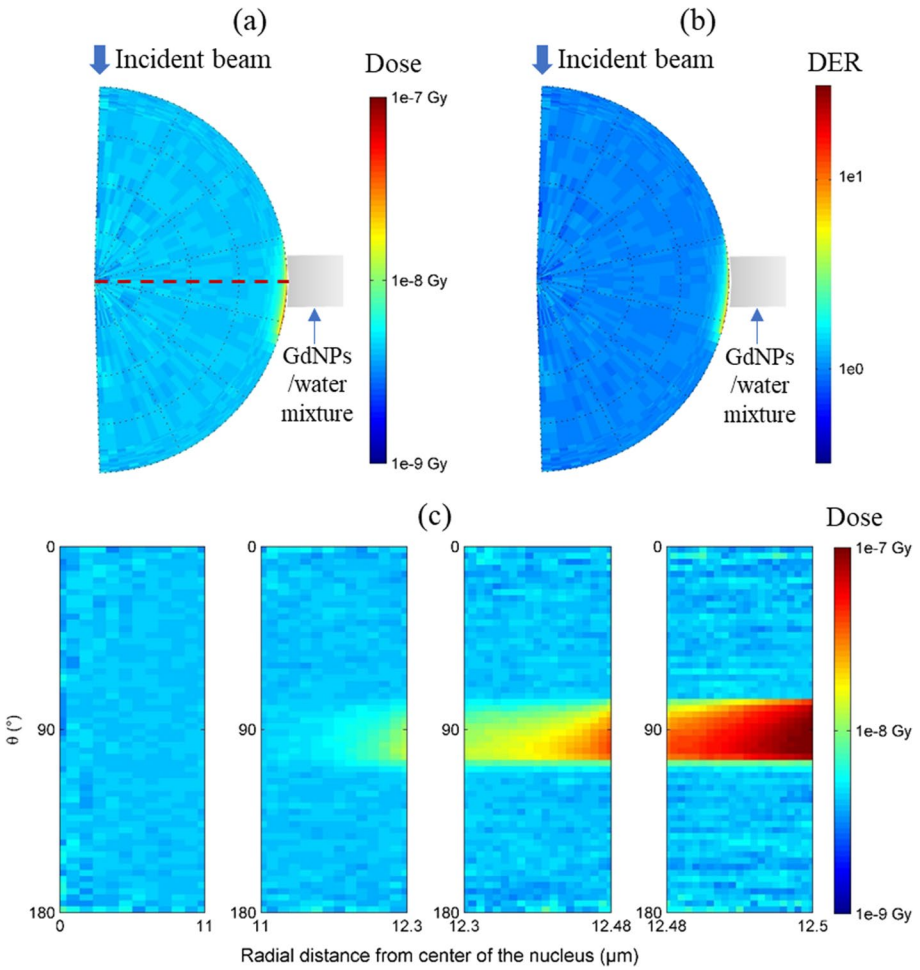

Fig. 8 Dose (**a**) and DER (**b**) distribution on half of the cross section in the nucleus for the irradiated cellular model, as shown in Fig. 4, and relationship between the dose distribution and radial distance from the center of the nucleus as well as the polar angle θ (**c**)

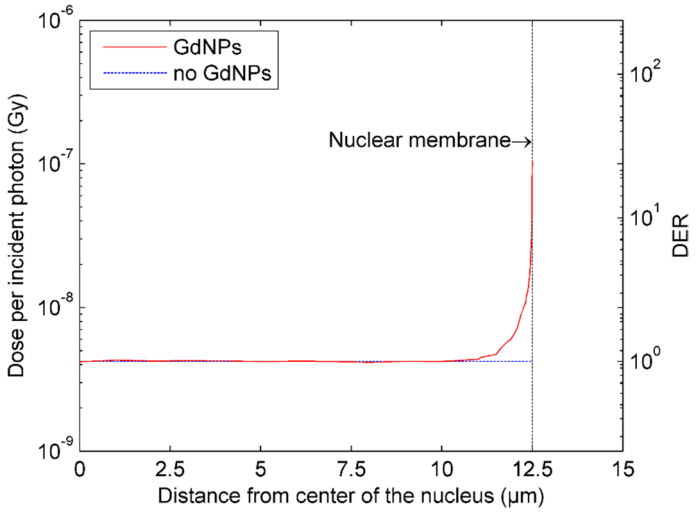

Fig. 9 Dose and DER profile along the 90-degree radial axis of the cross section of the nucleus

Simulations using the cellular model illustrated in Fig. 4 while changing the shell height to 15 μm were also conducted, and the results are shown in Additional file 1: Figs. S1 and S2.

Cell surviving fraction calculation

The predicted cell surviving fractions as a function of radiation dose using LEM is shown in Fig. 10. The experimental data for Panc1 tumor cells irradiated with and without GdNPs was also indicated for comparison (extracted from Detappe et al. 2015), as well as their LQM fittings. The fitting parameters (α and β) were 0.120 Gy^{-1} and 0.019 Gy^{-2} for cells incubated with AGuIX, and 0.070 Gy^{-1} and 0.019 Gy^{-2} without AGuIX. The α and β for cells incubated without AGuIX were used in LEM calculations.

For the dose range between 0 and 8 Gy, the deviations between the surviving fraction predictions and mean experimental results were all within 25%, and the surviving fraction predictions laid within one standard deviation of the experimental results. The experimental result for 10 Gy irradiation was an outlier and thus not taken into discussion. The predicted surviving fraction curve was fitted using the LQM shown in Eq. 6, and the derived DER_{eff} was 1.16. When the height of the partial shell was set to 15 μm in the simulation, the surviving fraction predictions were not comparable with the experimental results.

Discussion

In this study, the mechanism of radio-enhancement of GdNPs for kilovoltage photons was investigated using water cube phantom and cellular model. For single GdNP and clustered GdNPs irradiation in the water cube phantom, the secondary electron spectrum, dose distributions and DER distributions at nano-scale were calculated using MC simulations. For the cellular model containing GdNPs, the dose and DER distributions in the nucleus were simulated. LEM-based biological modeling of GdNP

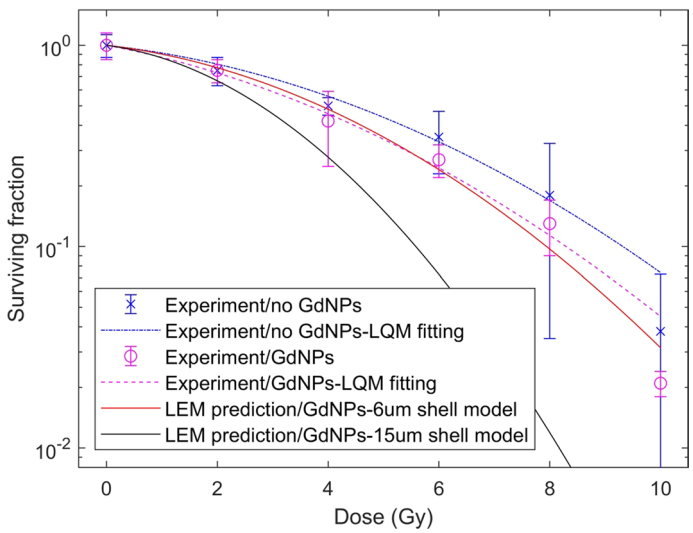

Fig. 10 Predicted cell surviving fractions using LEM. The experimental data with and without GdNPs was also indicated for comparison (extracted from Detappe et al. 2015), as well as their LQM fittings

radio-enhancement was established based on the nano-scale dose distributions in the nucleus, and the prediction of cell surviving fractions showed good agreement with experiment results.

Figure 5 and Table 1 show that the yield of electrons for GdNP was only 0.16% of the yield for GNP, whereas the average electron energy was 12% higher. The small proportion of gadolinium in GdNP and lower density of GdNP than GNP were the main causes for the low yield of electrons. The difference between the secondary electron spectra of GdNP and GNP was due to the different cross-sectional data and excitation energy of these two materials. Despite the large difference in the numbers of secondary electrons, the cellular uptake of AGuIX was orders of magnitude higher than that of GNPs (Yan et al. 2021), making the cellular contents of gadolinium and gold comparable. Compared to the dose distributions when GdNP was removed from water, GdNP enhanced dose around the particle evidently, as shown in Figs. 6 and 7. The dose per interacting photon at the surface of 5 nm GdNP was 28 times that of 50 nm GdNP, which was due to the self-shielding effect of nanoparticle clustering. In larger or clusters of GdNP, less electrons could escape from the GdNP as they would have to travel larger distances to escape compared to smaller GdNP. Similar dosimetric consequences of nanoparticle clustering have been elaborated for GNPs (Kirkby et al. 2017). In spite of the self-shielding effect, larger size of the GdNP leads to higher probability of interaction; thus, the DER of 50 nm GdNP was higher than 5 nm GdNP, as shown in Fig. 7. The dose enhancement by GdNP peaked at the particle surface (4.18 and 1.23 times for 50 nm and 5 nm GdNP, respectively) and declined rapidly with the increased distance from the surface. The majority of the dose enhancement was due to the contribution of Auger electrons, as shown in Fig. 6. The size of a single GdNP or clustering of GdNPs impacts the dose distribution pattern (the range and extent of dose enhancement) around the particle or cluster, as shown in Fig. 7. The DER at the surface of 50 nm GdNP was 3.42 times that for 5 nm GdNP. For the 5 nm GdNP, the radial DER maintained 1.1 or higher within a distance of 2 nm from the surface, whereas for the 50 nm GdNP this distance was increased to 27 nm. These properties of GdNPs were similar to those of GNPs (Engels et al. 2020).

The beam size of 1 μm utilized in the single GdNP irradiation study was large enough to reach electron equilibrium with respect to the Auger electrons released by the nanoparticles. To provide electron equilibrium with respect to the Compton interactions by the X-ray photons with the surrounding water medium, the beam size should be at least 288 μm, which would significantly increase the simulation workload. As the Auger electrons were dominant in the dose contribution, we considered that using the beam size of 1 μm would obtain simulation results with reasonable deviations. To verify this, radial dose for 50 nm GdNP was simulated using beam sizes of 1 and 2 μm, respectively, and a deviation within 5% was observed between the results.

Comparison between the secondary electron spectrum of GdNP and GNP irradiation suggested a larger range of dose enhancement near gadolinium than gold, which was consistent with McMahon's study. However, better secondary electron spectrum doesn't mean overall superiority. The radiosensitization effect in vitro or in vivo evolves many determinant factors, such as the physical and chemical properties of the nanoparticles, the uptake and distribution of the nanoparticles in the sub-cellular organelles, etc. This was beyond the research scope of this work and, therefore, not explored.

It is clearly shown that the dose deposition in the nucleus was concentrated in a ring close to the partial shell containing GdNPs. This is predictable as the dose enhancement by GdNP declines rapidly with the distance, as shown in Figs. 6 and 7. Furthermore, a large amount of aggregated GdNPs in the cellular model rendered a larger range of dose enhancement to the millimeter scale. This was also discovered in previous research on dose enhancement by GNPs (Engels et al. 2020). Besides, in this ring-shaped volume, the dose deposition has a broadening trend along the beam incident direction. This was mainly due to the uneven angular distribution of secondary electrons from the Compton scattering by GdNPs. The DER distribution has the same pattern as the dose distribution. The highest DER was about 26 at the nucleus surface, as shown in Fig. 9.

Although the largest deviation between the surviving fraction predictions and mean experimental results was 25%, all the surviving fraction predictions laid within one standard deviation of the experimental results. Therefore, it was considered a good agreement.

The difference between DER_{eff} (1.16) and DER_{av} (1.063) suggested that the uneven dose distribution in the sensitive volume significantly affects the biological effect of GdNP radiosensitization, and that the average dose in the sensitive volume cannot be used to evaluate the biological effect in this situation. This is consistent with previous findings for GNPs (Engels et al. 2020).

The distribution of nanoparticles in the cell should be considered carefully as it impacts the dose distribution calculation in the nucleus and thus the LEM-based surviving fraction prediction. Previous studies often used single nanoparticle (Ferrero et al. 2017) or homogeneously distributed nanoparticles (Brown and Currel 2017) in MC simulations for LEM calculation. Engels et al. used a partial shell-like configuration to mimic the unevenly distributed GNPs in the cytoplasm, and the LEM calculations matched the cell experiments well (Engels et al. 2020). The cell model used in this work was inspired by these previous studies and a good agreement with the experiments has been achieved. However, the geometry and sizes in this model may be quite different from realistic cell geometries. Changing the height of the partial shell would also have an evident impact on the dose distribution in the nucleus (comparing Figs. 8 and 9 with Additional file 1: Figs. S1 and S2) and thus the LEM-based prediction (Fig. 10). In fact, the height of the partial shell was set following previous study (Engels et al. 2020), but the pattern of nanoparticle distributions in the cytoplasm in this study should be different from theirs. More sophisticated cellular model mimicking the realistic cell geometries and GdNP distributions may be of interest in future works, and the validity of the approach in this work remains to be verified.

Literature has provided a wide range of α and β values for pancreatic cancer extracted from various clinical studies instead of determined values (Leeuwen et al. 2018). Therefore, the α and β values applied in this work were derived from the experimental data. Applying different α and β values may results in large deviations in LEM-based surviving fraction predictions and thus they should be carefully determined.

The methodology used in this study could be translated to other cell lines. The cell and nucleus shapes and sizes, nanoparticle uptake and intracellular distributions as well as the α and β values vary for other cell lines and should be determined based

on TEM observations, characterizations and experimental or clinical results before proper modeling.

This study considered only the physical dose enhancement in biological modeling, as it is the dominant mechanism of radiosensitization for kilovoltage photons. AGuIX has been used along with ^{192}Ir brachytherapy (average energy about 380 keV) to treat localized advanced cervical cancer in recent clinical trials (Lux et al. 2019). Similar model could be established in future studies to predict the biological effect. For other therapeutic rays, such as megavoltage photons and charged particles, the indirect radiation damage should be taken into account in future studies (Garty et al. 2010). For more comprehensive biological modeling of GdNP radio-enhancement, future studies should also consider more realistic cell geometric modeling, the influence from neighboring cells, as well as the disparity between cell lines.

Conclusions

The mechanism of radio-enhancement of GdNPs for kilovoltage photons was investigated using MC simulations. The yield of secondary electrons for GdNP was 0.16% of the yield for GNP, whereas the average electron energy was 12% higher. The majority of the dose enhancement was due to the contribution of Auger electrons. GdNP clusters had a larger range and extent of dose enhancement than single GdNPs, although GdNP clustering reduced radial dose per interacting photon significantly.

LEM-based biological modeling of GdNP radiosensitization was established based on the MC-calculated nano-scale dose distributions in a cellular model, and the prediction of cell surviving fractions showed good agreement with experimental results, although the deviation of simulation parameters can lead to large disparity in the results. To our knowledge, this was the first LEM-based biological model for GdNP radiosensitization.

Supplementary Information

The online version contains supplementary material available at https://doi.org/10.1186/s12645-023-00202-w.

Additional file 1: Figure S1. Doseand DERdistribution on half of the cross section in the nucleus for the irradiated cellular model as shown in Fig. 4, where the height of the partial shell was changed to 15 μm. Relationship between the dose distribution and radial distance from the center of the nucleus as well as the polar angle θ. **Figure S2.** Dose and DER profile along the 90-degree radial axis of the cross section of the nucleus for irradiated cellular model, as shown in Fig. 4, where the height of the partial shell was changed to 15 μm.

Acknowledgements
None.

Author contributions
JW conceived the idea, conducted the Monte Carlo simulation and wrote the main manuscript text. XX and YL helped in the data processing. TC did part of the literature review. EQ and LW revised the manuscript. All authors reviewed the manuscript. All authors read and approved the final manual script.

Funding
This work was supported by the National Natural Science Foundation of China (No. 12105367), National Cancer Center/National Clinical Research Center for Cancer/Cancer Hospital & Shenzhen Hospital, Chinese Academy of Medical Sciences and Peking Union Medical College, Shenzhen (No. E010322001), Shenzhen Science and Technology Program (No. JCYJ20220530153803008), Shenzhen Key Medical Discipline Construction Fund (No. SZXK013), Sanming Project of Medicine in Shenzhen (No. SZSM201612063) and Shenzhen High-level Hospital Construction Fund.

Availability of data and materials
The data that support the findings of this study are available from the corresponding author upon reasonable request.

Declarations

Ethicsapproval and consent to participate
Not applicable.

Consentfor publication
Notapplicable.

Competinginterests
Theauthors declare no competing interests.

Received: 12 October 2022 Accepted: 22 April 2023
Published online: 02 May 2023

References

Agostinelli S, Allison J, Amako K et al (2003) GEANT4—a simulation toolkit. Nucl Instrum Methods Phys Res A 506(3):250–303
Allison J et al (2006) Geant4 developments and applications. IEEE Trans Nucl Sci 53:270–278
Allison J, Amako K, Apostolakis J et al (2016) Recent developments in Geant4 nucl. Instrum. Methods Phys Res A 835:186–225
Brown JMC, Currell FJ (2017) A local effect model-based interpolation framework for experimental nanoparticle radiosensitisation data. Cancer Nanotechnol 8(1):1
Chandra RA, Keane FK, Voncken FEM, Thomas CR Jr (2021) Contemporary radiotherapy: present and future. Lancet 398(10295):171–184
Chatzipapas KP, Papadimitroulas P, Emfietzoglou D et al (2020) Ionizing radiation and complex DNA damage: quantifying the radiobiological damage using Monte Carlo simulations. Cancers (Basel) 12(4):799
Detappe A, Kunjachan S, Rottmann J et al (2015) AGuIX nanoparticles as a promising platform for image-guided radiation therapy. Cancer Nanotechnol 6(1):4
Du Y, Sun H, Lux F et al (2020) Radiosensitization effect of AGuIX, a gadolinium-based nanoparticle, in nonsmall Cell Lung Cancer. ACS Appl Mater Interfaces 12(51):56874–56885
Engels E, Bakr S, Bolst D et al (2020) Advances in modelling gold nanoparticle radiosensitization using new Geant4-DNA physics models. Phys Med Biol 65(22):225017
Ferrero V, Visonà G, Dalmasso F et al (2017) Targeted dose enhancement in radiotherapy for breast cancer using gold nanoparticles, part 1: a radiobiological model study. Med Phys 44(5):1983–1992
Garty G, Schulte R, Shchemelinin S et al (2010) A nanodosimetric model of radiation-induced clustered DNA damage yields. Phys Med Biol 55(3):761–781
Incerti S, Kyriakou I, Bernal MA et al (2018) Geant4-DNA example applications for track structure simulations in liquid water: a report from the Geant4-DNA project. Med Phys 45:e722–e739
Kempson I (2021) Mechanisms of nanoparticle radiosensitization. Wiley Interdiscip Rev Nanomed Nanobiotechnol 13(1):e1656
Kirkby C, Koger B, Suchowerska N et al (2017) Dosimetric consequences of gold nanoparticle clustering during photon irradiation. Med Phys 44(12):6560–6569
Lechtman E, Mashouf S, Chattopadhyay N et al (2013) A Monte Carlo-based model of gold nanoparticle radiosensitization accounting for increased radiobiological effectiveness. Phys Med Biol 58(10):3075–3087
Leeuwen CM, Oei AL, Crezee J et al (2018) The alfa and beta of tumours: a review of parameters of the linear-quadratic model, derived from clinical radiotherapy studies. Radiat Oncol 13(1):96
Liu R, Zhao T, Zhao X, Reynoso FJ (2019) Modeling gold nanoparticle radiosensitization using a clustering algorithm to quantitate DNA double-strand breaks with mixed-physics Monte Carlo simulation. Med Phys 46(11):5314–5325
Lux F, Tran VL, Thomas E et al (2019) AGuIX® from bench to bedside-transfer of an ultrasmall theranostic gadolinium-based nanoparticle to clinical medicine. Br J Radiol 92(1093):20180365
McMahon SJ (2018) The linear quadratic model: usage, interpretation and challenges. Phys Med Biol 64(1):01TR01
McMahon SJ, Paganetti H, Prise KM (2016) Optimising element choice for nanoparticle radiosensitisers. Nanoscale 8(1):581–589
Perl J, Shin J, Schumann J, Faddegon B, Paganetti H (2012) TOPAS: an innovative proton Monte Carlo platform for research and clinical applications. Med Phys 39(11):6818–6837
Poludniowski G, Omar A, Bujila R, Andreo P (2021) Technical note: SpekPy v2.0-a software toolkit for modeling X-ray tube spectra. Med Phys 48(7):3630–3637
Rudek B, McNamara A, Ramos-Méndez J et al (2019) Radio-enhancement by gold nanoparticles and their impact on water radiolysis for X-ray, proton and carbon-ion beams. Phys Med Biol 64(17):175005
Scholz M, Kraft G (1993) Calculation of heavy ion inactivation probabilities based on track structure, X Ray sensitivity and target size. Radiat prot dosim 1:29–33
Schuemann J, McNamara AL, Ramos-Méndez J et al (2019) TOPAS-nBio: an extension to the TOPAS Simulation toolkit for cellular and sub-cellular radiobiology. Radiat Res 191(2):125–138
Sung H, Ferlay J, Siegel RL et al (2021) Global cancer statistics 2020: GLOBOCAN estimates of incidence and mortality worldwide for 36 cancers in 185 countries. CA Cancer J Clin 71(3):209–249
Taupin F, Flaender M, Delorme R et al (2015) Gadolinium nanoparticles and contrast agent as radiation sensitizers. Phys Med Biol 60(11):4449–4464
Verry C, Sancey L, Dufort S et al (2019) Treatment of multiple brain metastases using gadolinium nanoparticles and radiotherapy: NANO-RAD, a phase I study protocol. BMJ Open 9(2):e023591

Verry C, Dufort S, Lemasson B et al (2020) Targeting brain metastases with ultrasmall theranostic nanoparticles, a first-in-human trial from an MRI perspective. Sci Adv 6(29):eaay5279
Wu J, Xie Y, Wang L, Wang Y (2020) Monte Carlo simulations of energy deposition and DNA damage using TOPAS-nBio. Phys Med Biol 65(22):225007
Xu X, Wu J, Dai Z et al (2022) Monte Carlo simulation of physical dose enhancement in core-shell magnetic gold nanoparticles with TOPAS. Front Oncol 12:992358
Yan H, Carlson DJ, Abolfath R, Liu W (2021) Microdosimetric investigation and a novel model of radiosensitization in the presence of metallic nanoparticles. Pharmaceutics 13(12):2191

Publisher's Note